Ab initio and empirical-potential studies of defect properties in 3*C*-SiC

Fei Gao,* Eric J. Bylaska, William J. Weber, and L. René Corrales
Pacific Northwest National Laboratory, P.O. Box 999, Richland, Washington 99352
(Received 25 April 2001; revised manuscript received 16 August 2001; published 4 December 2001)

Density functional theory (DFT) is used to study the formation and properties of native defects in 3*C*-SiC. Extensive calculations have been carried out to determine the formation of point defects and the stability of self-interstitials. Although there is good agreement in the formation of vacancies and antisite defects between the present study and previous calculations, a large disparity appears in the formation of self-interstitials. The most favorable configurations for *C* interstitials are ⟨100⟩ and ⟨110⟩ dumbbells, with formation energies from 3.16 to 3.59 eV, and the most favorable Si interstitial is Si tetrahedral surrounded by four C atoms, with a formation energy of 6.17 eV. The present DFT results are also compared with those calculated by molecular dynamics (MD) simulations using the Tersoff potentials, with parameters obtained from the literature. The formation energies of vacancies and antisite defects obtained by MD calculations are in good agreement with those obtained by DFT calculations. However, the MD calculations yield different results for interstitials energies and structures that depend on the cutoff distances used in the Tersoff potentials. The results provide guidelines for evaluating the quality and fit of empirical potentials for large-scale simulations of irradiation damage and defect migration processes in SiC.

DOI: 10.1103/PhysRevB.64.245208 PACS number(s): 71.15.Pd, 61.72.Ji, 61.82.Fk, 31.15.Ar

I. INTRODUCTION

Materials and devices based on silicon carbide (SiC) have been considered as potential candidates for high-temperature, high-frequency, and high-power applications because of their high thermal conductivity, high electron mobility, high electron saturation velocity, and wide band gap. These excellent properties make SiC suitable for direct process monitoring in the aerospace, petrochemical, food processing, automotive, and nuclear industries.[1] Experimental results on SiC have indicated that point defects may enhance dopant diffusion rates and, thus, affect the overall performance of SiC-based semiconductor devices. Therefore, it is clear that defects play a very important role in mediating self-diffusion and the diffusion of substitutional impurities. SiC has also been recognized as a potential cladding material for gas-cooled fission reactors,[2] structural components for fusion reactors,[3] and an inert matrix for the transmutation of plutonium[4] because of its small neutron-capture cross section, low activation, and good thermal conductivity under irradiation. The defects created by energetic displacement cascades during ion implantation or neutron irradiation and their subsequent evolution give rise to important microstructural changes that affect many of the macroscopic properties of electronic devices and nuclear components. Determination of defect formation and energetics is therefore crucial for understanding the response of SiC to self-diffusion, diffusion of substitutional impurities, radiation damage, and ion implantation.

There have been many studies of defect energetics in 3*C*-SiC using both the *ab initio* method[5,6] and molecular dynamics (MD).[7] The *ab initio* calculations by Wang *et al.*[5] used a very small number of atoms to study interstitials. It is believed that a full three-dimensional relaxation was not achieved, particularly with respect to interstitial formation.[5] Although a supercell of up to 128 atoms was used by Torpo *et al*. to determine the properties of native defects in 3*C*- and 2*H*-SiC, only a subset of possible defects was investigated.[6] Empirical potentials have also been employed to calculate point-defect properties in SiC.[7] However, considerable ambiguity has been introduced into the literature regarding the formation of native defects, their clustering, and in particular the stability of interstitial configurations because different empirical potentials lead to different results. Although extensive efforts have been carried out in order to understand the fundamental issues of ion-solid interactions in SiC,[8–11] key questions about defect properties are yet unanswered.

Density functional theory (DFT) calculations require large computational efforts compared to the large-scale computer simulations normally applied to ion-solid interactions. Molecular dynamics simulations using empirical potentials are commonly employed to study displacement cascades and have been applied to a wide range of materials, including metals[12,13] and ceramics.[8–11,14] However, *ab initio* calculations can provide a set of accurate defect formation energies as well as guidelines for evaluating the quality and fit of empirical potentials. In this study, DFT calculations are used to study the formation energies of monovacancies, antisite defects, and possible interstitial configurations. Based on the results, the relative stability of various interstitial configurations is determined. In parallel, MD simulations using a modified Tersoff potential, with different cutoff distances and parameters obtained from the literature, have also been employed to obtain point defect properties in 3*C*-SiC. The MD results are compared with those obtained using DFT and with those obtained by others. In addition, the understanding of native defect properties undertaken in this study is complementary to the extensive MD simulations previously reported.[8–11]

II. *Ab initio* CALCULATIONS

A. Method

The density functional theory calculations are based on the pseudopotential plan-wave method within the framework

of the local density approximation (LDA). A parametrized form of the exchange-correlation potential obtained by Vosko *et al.*[15] is used. This functional is based upon an exact solution of the electron gas from the quantum Monte Carlo calculations of Ceperley and Alder.[16] This local density functional is quite robust and contains within its limits earlier functionals based on the high-density limit of the electron gas obtained by Gell-Mann and Bueckner,[17] as a well as the low-density limit of the electron gas obtained by Wigner.[18] Experience has shown that local density functionals agree quite well with experiment in predicting structural parameters and harmonic constants for a variety of chemical and solid-state systems.[19] Even though local density functionals exhibit systematic over binding, for relative energy calculations the errors are often significantly smaller.[20] The valence electron interactions with the atomic core are approximated with a generalized norm-conserving pseudopotential developed by Hamann[21] and modified to a separable form suggested by Kleinman and Bylander.[22] The original pseudopotential parametrization suggested by Hamann is too ''hard'' for carbon and requires a large number of plane waves. A softer pseudopotential, constructed by increasing the core radii ($r_{cs}=0.80$ a.u., $r_{cp}=0.85$ a.u., and $r_{cd}=0.85$ a.u.), is used to reduce the number of plane waves needed to describe the carbon pseudopotential. Carbon cluster calculations by Brabec *et al.*[23] and Bylaska *et al.*[24–26] have shown that this softened carbon pseudopotential produces reliable results at reasonable plane-wave basis-set sizes. All calculations are performed at the Γ point. A plane-wave basis set with a cutoff energy of 36 Ry (980 eV) is used to expand the electronic wave functions, but a large plane-wave energy of cutoff of 86 Ry (2340 eV) has been checked in many cases. Basis-set errors associated with a small basis are reasonable, with the large basis stabilizing the defects by at most 0.2 eV in all cases. The lattice constant, bulk modulus, and cohesive energy obtained using a 36-Ry cutoff energy and these pseudopotentials for an eight-atom unit cell of SiC are 0.438 nm, 2.22 Mbar, and 6.58 eV, respectively, in $3C$-SiC, which are in excellent agreement with experimental data[27] and other DFT calculations.[5,28] Typically, the calculations are performed in 32-, 64-, and 128-atom unit cells with a fixed volume (lattice constant of 0.438 nm), depending on defect configurations. In order to test size effects on the defect formation energy, a 68-atom or 128-atom supercell has been used to calculate the C^+-C$\langle 100\rangle$ dumbbell, and the results show that the formation energy is 3.16 and 3.09 eV for 68- and 128-atom supercells, respectively. The error associated with the two different supercells is on the order of 0.07 eV. To avoid any spurious symmetries, the initial atomic configurations have been randomized slightly from the ideal structure, and all ions in the supercell have been allowed to relax without any symmetry constraints.

The results for vacancies and antisite defects are obtained using a 32-atom supercell, while 64-atom and 128-atom supercells are used to calculate interstitials. The conjugate gradient (CG) method for Grassman manifolds[29] is used to minimize the wave function of electrons, and the minimum and metastable structures are optimized using a Broyden-Fletch-Goldfarb-Shanno quasi-Newton algorithm with analytic gradients. The structural optimization is stopped when maximum force per atom is less than 1×10^{-4} a.u.

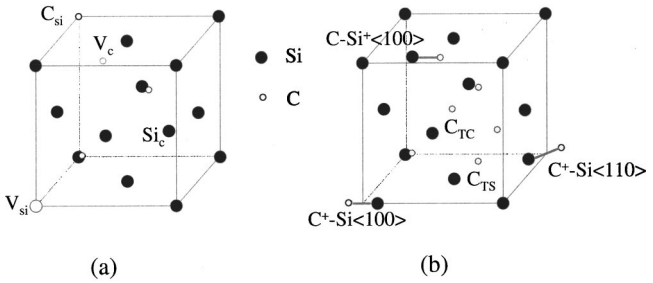

FIG. 1. Schematic illustration of (a) vacancies and antisite defects and (b) the possible interstitials that may exit in 3C-SiC.

For a two-element system, there are a number of possible references to obtain the total energy of a system in *ab initio* calculations. To simplify this, isolated C and Si atoms (calculated using a large fcc supercell with lattice constant of 38 a.u.) at the same cutoff energy as the crystal were chosen as a reference to evaluate the total energy of the crystal in the ground state. The formation energy for a vacancy can be defined as[30]

$$E_f^{\nu}=\Delta E^{\nu}(X)+\varepsilon, \tag{1}$$

and, for an antisite defect,

$$E_f(X_Y)=\Delta E(X_Y), \tag{2}$$

where X and Y represent C or Si species, and ε is the negative cohesive energy in a perfect crystal of $3C$-SiC in the ground state. ΔE denotes the total energy difference between the crystal containing a defect and the perfect crystal with the same number of lattice sites. To be consistent with the vacancy and antisite defect calculations, the formation energy of an interstitial is given by

$$E_f^i(X)=\Delta E^i(X)-\varepsilon, \tag{3}$$

where ΔE again is the total energy difference between the crystal containing an interstitial and that of the perfect crystal with the same number of lattice sites.

B. Formation energies of defects

In $3C$-SiC, there are two types of vacancies: namely, the C and Si vacancies with four Si or four C atoms as nearest neighbors, respectively. Besides these vacancies, there are two types of antisite defects, formed by atoms located on the wrong sublattice. These defects are shown in Fig. 1(a), where Si_C represents a silicon atom on a carbon site and C_{Si} a carbon atom on a silicon site. For self-interstitial defects, there are ten possible structures, as indicated in Fig. 1(b). A carbon tetrahedral interstitial has two different configurations, depending on the arrangement of neighbor atoms such that C_{TS} is surrounded by four Si atoms and C_{TC} by four C atoms. The other tetrahedral interstitials are Si_{TS}, with four Si atoms as nearest neighbors, and Si_{TC}, with four C atoms. There are four possible $\langle 100\rangle$ dumbbell configurations. Two are C^+-Si and Si^+-Si pairs centered on

TABLE I. The formation energy of vacancies, antisite defects, and interstitials calculated by *ab initio* methods.

Defects	Formation energy (eV)	
	Ab initio (Ref. 5)	*Ab initio* (present work)
V_C	5.90	5.48
V_{Si}	6.80	6.64
C_{Si}	1.10	1.32
Si_C	7.30	7.20
C_{TC}	11.0	6.41
C_{TS}	8.6	5.84
Si_{TC}	14.7	6.17
Si_{TS}	15.0	8.71
C^+-Si⟨100⟩		3.59
C^+-C⟨100⟩		3.16
Si^+-C⟨100⟩		10.05
Si^+-Si⟨100⟩		9.32
C^+-C⟨110⟩		3.32
C^+-Si⟨110⟩		3.28

Si sites, and the other two are C^+-C and Si^+-C pairs centered on C sites, where the superscript plus indicates the interstitial atom. The other atom is the atom that initially occupied the site. Besides these tetrahedral and ⟨100⟩ dumbbell configurations, it is also possible to have two ⟨110⟩ dumbbell configurations: namely, C^+-C⟨110⟩ and C^+-Si⟨110⟩ dumbbells.

The formation energies of vacancies, antisite defects, and interstitials are listed in Table I, together with previous *ab initio* calculations[5] for comparison. The formation energies of C and Si vacancies are 5.48 and 6.64 eV, respectively, and the formation energies of C_{Si} and Si_C are 1.32 and 7.20 eV, respectively. Wang, Bernholc, and Davis[5] used a similar *ab initio* method, but different exchange-correlation potential, to calculate a subset of native defects in 3*C*-SiC. With a 32-atom supercell, they found that the formation energies are 5.9, 6.8, 1.1, and 7.30 eV for V_C, V_{Si}, C_{Si}, and Si_C respectively. The present formation energies are in good agreement with their results, which suggests that the effects of exchange-correlation potentials on defect formation are very small. A large difference appears in the interstitial calculations, particularly associated with the stability of interstitials. The results obtained by Wang *et al.*[5] give generally high formation energies, which may be due to the small number of atoms in their calculations (16 atoms for interstitial calculations) and the difficulty in achieving full relaxation. Recently, Torpo *et al.*[6] reported on *ab initio* results for native defects in 3*C*-SiC, but only a small subset of possible defects was studied. According to their calculations, the interstitials in the tetrahedral sites of C_{TS} and Si_{TS} form high-energy configurations, and the estimated formation energy of the C_{TC} interstitial is about 7 eV. The present results are in good agreement with their calculations. In the present study, the most favorable configuration for C interstitials are ⟨100⟩ and ⟨110⟩ dumbbells, with formation energies from 3.16 to 3.59 eV. It is interesting to note that the two atoms in the ⟨110⟩ dumbbells have undergone a shift along the direction

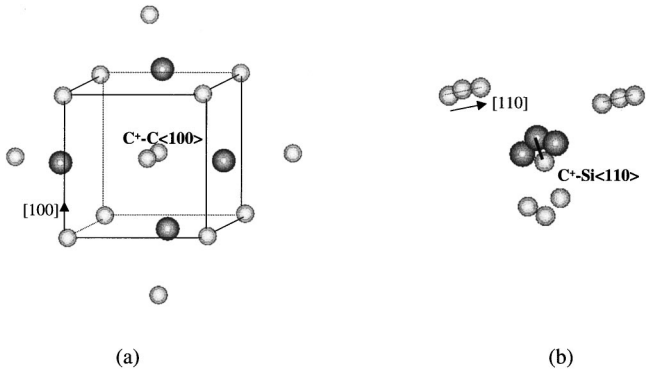

FIG. 2. The defect configurations and atomic relaxation for (a) the C^+-C⟨100⟩ and (b) C^+-Si⟨110⟩ interstitials obtained by *ab initio* calculations.

perpendicular to dumbbell's axis, and the shifting distances are, for instance, about 0.027 and −0.025 nm for C and Si atoms in a C^+-Si⟨110⟩ dumbbell, respectively. The local atomic structures of the C^+-C⟨100⟩ and C^+-Si⟨110⟩ dumbbells are shown in Fig. 2, where large spheres represent Si atoms and small spheres C atoms. The shifts of C and Si atoms can be clearly seen in Fig. 2(b), but no atomic displacements are found along the ⟨001⟩ direction for ⟨100⟩ dumbbells [Fig. 2(a)]. In the case of Si interstitials, the most favorable configuration is the Si tetrahedral surrounded by four C atoms, with a formation energy of 6.17 eV.

C. Charge density distribution

As described above, the lowest-energy configuration for a C interstitial is the C^+-C⟨100⟩ dumbbell centered at a C site. Its charge density in a (001) C plane is shown in Fig. 3, where interstitial atoms are indicated by the solid circles.

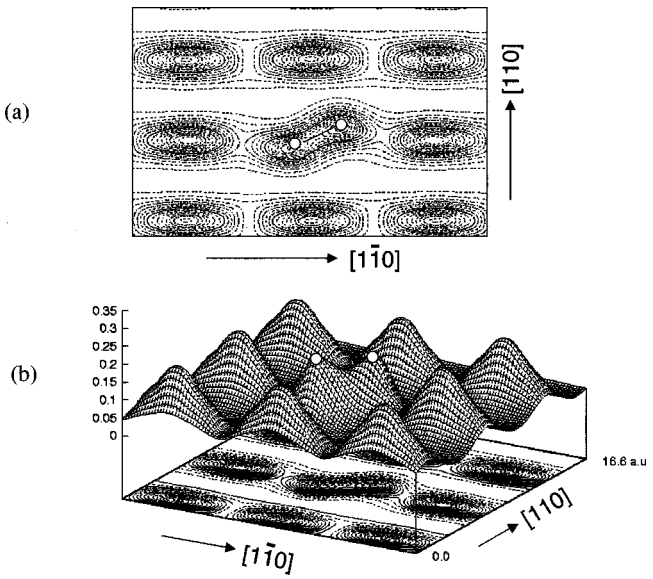

FIG. 3. (a) The charge density (a.u.) contour plot and (b) the charge density surface distribution on the [001] carbon plane for the C^+-C⟨100⟩ dumbbell. The positions of two atoms in the dumbbell are indicated by the solid circles.

Figure 3(a) shows a contour plot of the charge density, while Fig. 3(b) represents the surface plot of the charge density in the (001) C plane. In this configuration, the C atoms are displaced along the ⟨100⟩ direction about 0.064 nm, giving a bond distance of 0.129 nm. The bond distance of C^+-C dumbbell is about 32% smaller than the normal Si^+-C bond length of the first neighbor, resulting in the formation of a strong bond. It is also clear from Figs. 3(a) and 3(b) that more charge density distributes along the bond directions rather than centered at atoms. The charge transfer from atoms to the bonding region results in a decrease of the total energy, which gives a decrease in the formation energy of the C^+-C⟨100⟩ dumbbell. It is found that the Si atoms of the first-neighbor shell relax largely outward, about 18.2% of the bond distance away from their respective lattice sites. The C atoms of second-neighbor shell in the planes, which contain the dumbbell, relax also slightly outward, about 1.3% of the bond distance, while the positions of C atoms in the plane perpendicular to the dumbbell's axis are the same as their respective lattice sites, without any relaxation.

Although a strong bond is formed in the case of the C^+-Si⟨110⟩ dumbbell centered at a Si site, with a bond distance of 0.131 nm, the distortion of surrounding atoms is quite large. The large distortion is due to the small size of the C lattice site. Both the first-neighbor (Si atom) and second-neighbor (C atom) shells relax outward about 18.2% and 1.3% of the bond distance away from their lattice sites. This is consistent with the formation energy of the C^+-C ⟨110⟩ dumbbell being slightly higher than that of the C^+-Si ⟨110⟩ interstitial. Turning to the C_{TS} interstitial, its bond length with surrounding Si atoms is found to be 0.201 nm, which is about 5.7% longer than the normal Si-C bond length. Its charge density along the $(1\bar{1}0)$ plane is plotted in Figs. 4(a) and 4(b), where the position of the C interstitial is also indicated by the solid circle. These plots, together with their bond length, clearly show that the C_{TS} interstitial forms a weak bond, giving a higher formation energy in comparison with C^+-Si⟨110⟩ and C^+-C⟨110⟩ interstitials. The relaxation of the Si atoms in the first-neighbor shell is about 4.6% of the normal bond distance outward, and there is almost no relaxation on C atoms of the second-neighbor shell.

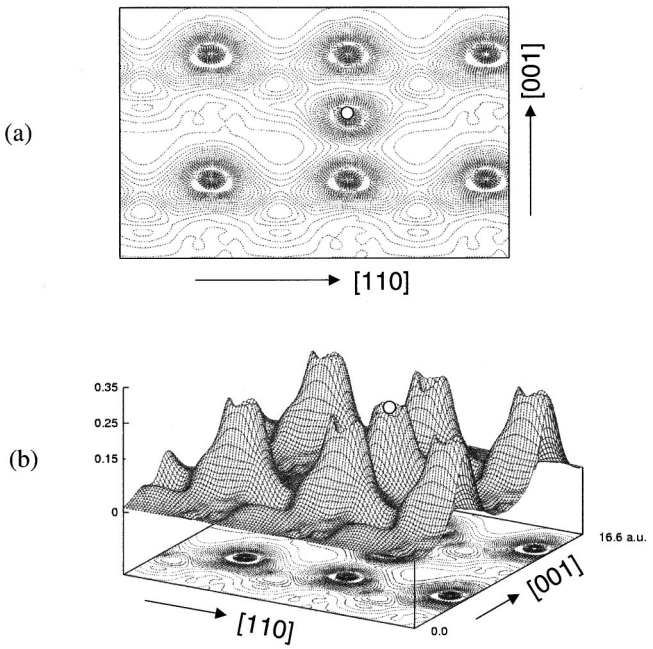

FIG. 4. (a) The charge density (a.u.) contour plot and (b) the charge density surface distribution on the $[1\bar{1}0]$ plane for the C_{TS} interstitial. The position of the interstitial is indicated by the solid circle.

III. MD CALCULATIONS WITH TERSOFF POTENTIALS

A. Method

The Tersoff potentials with different parameter sets[31,32] are used in the MD simulations to determine the energetics and nature of defect formation in SiC. The potential is composed of repulsive and attractive interactions given by

$$E=\frac{1}{2}\sum_{i\neq j} f_c(r_{ij})[A_{ij}\exp(-\lambda_{ij}r_{ij})-b_{ij}B_{ij}\exp(-\mu_{ij}r_{ij})], \tag{4}$$

where b_{ij} is the bond order described by

$$b_{ij}=\chi_{ij}(1+\xi_{ij}^{n_i})^{-1/2n_i}. \tag{5}$$

The parameter of $\xi_{ij}^{n_i}$ is the same as that given in Ref. 31. The cutoff function is given by

$$f_c(r_{ijj})=\begin{cases}1, & r_{ij}\leqslant R_{ij},\\ 0.5+0.5\cos\left[\pi\dfrac{r_{ij}-R_{ij}}{S_{ij}-R_{ij}}\right], & R_{ij}<r_{ij}\leqslant S_{ij},\\ 0, & r_{ij}>S_{ij},\end{cases} \tag{6}$$

where A_{ij} and B_{ij} are constant parameters of Morse potentials, and S_{ij} and R_{ij} are the parameters such that $f_c(r)$ has continuous values and derivatives for all r and goes from 1 to 0. Here R_{ij} is chosen to include only the first-neighbor shell of SiC. The standard mixing rules are used such that the parameters λ_{ij} and μ_{ij} are arithmetic averages, and A_{ij}, B_{ij}, R_{ij}, and S_{ij} are geometric averages of the corresponding single component i and j values. One set of parameters for the Tersoff potentials for SiC is from Devanathan *et al.*[33] These potentials have been further modified to match *ab initio* calculations for short-range interactions.[33] This set of parameters and cutoffs, labeled as TPA, has been employed to calculate defect properties,[7] displacement threshold energies[33] (E_d), and 10-keV displacement cascades[9] in $3C$-SiC. Another set of cutoff distances with the same potential parameters,[34] labeled as TPB, have been used to evaluate E_d and to simulate displacement cascades in the energy range from 0.5 to 8 keV.[34] However, no information on defect properties using the TPB parameters was reported. Both sets of cutoff parameters are listed in Table II. The properties of various point defects have been determined by MD simulations with these potentials. The simulations are

TABLE II. The parameters of the cutoff function employed in the present study.

	C-C[a]	C-Si[a]	Si-Si[a]	C-C[b]	C-Si[b]	Si-Si[b]
R_{ij} (nm)	0.18	0.220454	0.27	0.220454	0.220454	0.220454
S_{ij} (nm)	0.21	0.250998	0.3	0.250998	0.250998	0.250998

[a]The parameters used in Ref. 7.
[b]The parameters used in Ref. 34.

carried out in a cubic box of 1000 unit cells consisting of 8000 atoms with periodic boundary conditions and constant pressure relaxations at a temperature of 0 K.

B. Results and discussion

The formation energies of vacancies, antisite defects, and interstitials calculated using the TPA and TPB potentials, described above, are listed in Table III. It is important to note that the formation energies of E_f^v(C) and E_f^v(Si) obtained using TPA MD are 5.20 and 6.31 eV, respectively, which are in excellent agreement with those determined using DFT. These values are also in good agreement with the calculated values using TPB MD. Huang *et al.*[7] used the same Tersoff potential with similar parameters and cutoffs in Ref. 9 to calculate defect properties. They obtained formation energies for C and Si vacancies of 5.18 and 6.01 eV, respectively. All calculations described above give similar values for formation energies of vacancies in $3C$-SiC. The difference between E_f^v(Si) and E_f^v(C) is about 1.11 and 1.16 eV by TPA and TPB, respectively, and about 1.16 eV by *ab initio* calculations. This demonstrates that the vacancy properties in SiC can be well described by the Tersoff potentials for both parameter sets used in this work.

TABLE III. The formation energy of interstitials calculated by MD methods, where TPA-MD represents the MD calculations with potential parameters used in Ref. 7 and TPB-MD in Ref. 34.

	Formation energy (eV)	
Defects	TPA-MD	TPB-MD
V_C	5.20	5.15
V_{Si}	6.31	6.31
C_{Si}	0.35	0.35
Si_C	6.10	5.50
C_{TC}	4.86	8.34
C_{TS}	2.51	6.68
Si_{TC}	15.18	10.52
Si_{TS}	14.64	14.33
C^+-Si$\langle 100\rangle$	9.03	5.88
C^+-C$\langle 100\rangle$	6.41	5.97
Si^+-C$\langle 100\rangle$	9.10	11.28
Si^+-Si$\langle 100\rangle$	15.44	10.03
C^+-C$\langle 110\rangle$	6.21	6.50
C^+-Si$\langle 110\rangle$	[a]	9.39

[a]Unstable: converts to a C^+-C$\langle 110\rangle$ dumbbell.

For the antisite defects Si_C and C_{Si}, the formation energies given by the TPA-MD simulations are 6.1 and 0.35 eV compared with 7.20 and 1.32 eV calculated by the *ab initio* method in the present study. It can be seen that large differences appear in the formation energies of antisite defects, denoting a clear distinction between the two sets of calculations. The larger value given by both MD and *ab initio* calculations for the Si_C antisite defect has a simple physical interpretation in that a small C atom is replaced by a large Si atom. This may suggest that the defect properties in SiC are strongly influenced by the relative sizes of the atomic species. Nevertheless, the large energy increase in forming an antisite defect pair, predicted by both *ab initio* DFT calculations and MD simulations, implies that the $3C$-SiC structure may be thermally stable against the formation of highly disordered structures.

With regard to interstitial properties, it should be noted that there is an extensive study of interstitial properties previously in $3C$-SiC by Huang *et al.*,[7] using three representative empirical potentials. In the present study, the same parameters and cutoff distances for the Tersoff potentials have been employed to calculate interstitials properties, but the results of the previous study[7] could not be reproduced here. The formation energies calculated by MD simulations with TPA and TPB potentials are also listed in Table III.

In general, there is a reasonable agreement between DFT calculations and the TPB-MD results, but there is a large disparity between the TPA-MD and DFT studies, particularly for C interstitials. However, it is of interest to note that all calculations consistently give a lower formation energy for C interstitials than for Si interstitials. For the four possible configurations of the C interstitial, the C^+-Si$\langle 100\rangle$ and C^+-C$\langle 100\rangle$ dumbbells shown in Fig. 1(b) are the most favorable configurations in the TPB-MD calculations, having the formation energy of 5.88 and 5.97 eV, respectively. Any configuration of the C interstitials that are in tetrahedral positions (TS or TC) appear energetically unfavorable and may be unstable with respect to conversion back to the C^+-C$\langle 100\rangle$ or C^+-Si$\langle 100\rangle$ dumbbells at higher temperatures in the TPB-MD calculations. As described above, the most favorable configurations for C interstitials obtained by DFT calculations is $\langle 100\rangle$ and $\langle 110\rangle$ dumbbells centered at a C site or a Si site. This disparity in the stability of interstitials marks a real distinction between MD and DFT calculations. An analysis of the charge density distribution and the bond length of the interstitials presented above indicates that both $\langle 100\rangle$ and $\langle 110\rangle$ dumbbells form a strong bond, with a bond length 32% and 15% shorter than the normal Si-C bond length, respectively, whereas the C_{TS} interstitial forms a weak bond with Si atoms that are about 5.7% longer than the normal Si-C bond. The charge transfer from atoms to the bonding region results in a decrease of the total energy, which yields the smaller formation energies for $\langle 100\rangle$ and $\langle 110\rangle$ dumbbells compared to tetrahedral interstitials.

In the TPA-MD simulations, two C tetrahedral interstitial configurations become energetically favorable, in contrast to those determined by the *ab initio* and TPB-MD methods. The C_{TS} interstitial forms the most stable configuration with the formation energy of only 2.51 eV, which is much lower than

other interstitials. The stable interstitials in the DFT and TPB-MD calculations—namely, C^+-Si⟨110⟩ and C^+-C⟨110⟩ dumbbells—become metastable configurations that can convert to a C_{TS} configuration in the TPA-MD model.

Although there is a large disparity in the formation of C interstitials between the TPA-MD and both the DFT and TPB-MD results, all calculations are in agreement with respect to the Si interstitials, giving a generally higher formation energy. This is expected because of the size difference between Si and C atoms. For example, the tetrahedral interstitial cavity has a small volume with the radius of 0.094 nm, compared to the covalent radius of the Si atom (0.118 nm). In the TPA-MD model, all Si interstitials are found to be unstable with respect to conversion to a Si_C antisite defect plus a C_{TS} interstitial, since the formation energy of the latter pair is about 8.61 eV. This does not occur in the TPB-MD and DFT calculations.

The stability of interstitials is an important issue because of its influence on materials properties in several major areas, such as mechanical, electrical, and dimensional properties. Our particular interest in this area is to study the creation of point defects in SiC by ion-solid interactions. It is not clear to what extent a more accurate description of the interatomic potential would affect the production of defects by the cascade process. Devanathan *et al.*[35] employed the TPA-MD method to study the Si displacement cascades in energy from 250 eV to 30 keV in 3*C*-SiC, and the results show the average number of interstitials generated to be about 50 for cascades of 5 keV recoils. In another extensive study of defect production in 3*C*-SiC that employed the TPB-MD method,[34] the average number of interstitials produced in 5 keV cascades is about 49, which is in excellent agreement with that obtained by Devanathan *et al.*[35] Therefore, it seems reasonable that a more accurate potential with respect to containing all physics would not seriously affect in-cascade defect production and survival, particularly to those at low temperatures, since the thermal spike in SiC is very short.[9,10] However, it is expected that the nature of the potential will have a more significant influence on the mobility of self-interstitial atoms and their clustering. The development of more accurate potentials that match to DFT calculations would provide for more accurate MD simulations of defect migration and cascade annealing processes, which is the direction of our current research efforts.

IV. SUMMARY

Both DFT calculations and MD simulations have been used to study the formation energies and properties of native defects in 3*C*-SiC. In general, the formation energies of vacancies and antisite defects determined by MD simulations with the Tersoff potentials, regardless of the cutoff distances, are in good agreement with those determined by DFT calculations. Although there is a large disparity for C interstitials between the TPA-MD and both the DFT and TPB-MD calculations, these methods yield very similar results and trends for the Si interstitials, which have generally higher formation energies. DFT calculations show that the most favorable C interstitial configurations are ⟨100⟩ and ⟨110⟩ dumbbells centered at a C site or a Si site. This may be due to the charge transfer from atoms to the bonding region, resulting in the formation of a strong bond. In the case of the Si interstitial, the most favorable configuration is the Si tetrahedral surrounded by four C atoms. However, the TPB-MD calculations give the C^+-Si⟨100⟩ and C^+-C⟨100⟩ dumbbells as the most favorable configurations, while the TPA-MD model gives the C_{TS} interstitial as the most stable configuration, in marked contrast with the DFT results. Both DFT and TPB-MD results predict that any configurations of C interstitials based on tetrahedral positions TS or TC are energetically unfavorable and may be unstable with respect to conversion back to C^+-Si⟨110⟩ and C^+-Si⟨100⟩ dumbbells at higher temperature, respectively.

ACKNOWLEDGMENTS

This research was supported by (F.G. and W.J.W.) the Division of Materials Sciences and Engineering, Office of Basic Energy Sciences, U.S. Department of Energy, (E.J.B.) Environmental Molecular Science Laboratory operations, which are supported by the Office of Biological and Environmental Research, (U.S.) Department of Energy, and (L.R.C.) the Division of Chemical Sciences, Office of Basic Energy Sciences, U.S. Department of Energy. We also wish to thank the Scientific Computing Staff, Office of Science, U.S. Department of Energy for a grant of computer time at the National Energy Research Scientific Computing Center (Berkeley, CA), which is supported by the Office of Science, U.S. Department of Energy. Pacific Northwest National Laboratory is operated by Battelle for the U.S. Department of Energy under Contract No. DE-AC06-76RLO 1830.

*Corresponding author. FAX: 1-509 376 5106. Electronic address: fei.gao@pnl.gov

[1] M. A. Capano and R. J. Trew, MRS Bull. **22(3)**, 19 (1997).
[2] B. G. Kim, Y. Coi, J. W. Lee, Y. W. Lee, D. S. Sohn, and G. M. Kim, J. Nucl. Mater. **281**, 163 (2000).
[3] P. Fenici, A. J. F. Rebelo, R. H. Jones, A. Kohyama, and L. L. Snead, J. Nucl. Mater. **258**, 215 (1998).
[4] R. A. Verrall, M. D. Vlajic, and V. D. Krstic, J. Nucl. Mater. **274**, 54 (1999).
[5] C. Wang, J. Bernholc, and R. F. Davis, Phys. Rev. B **38**, 12 752 (1988).
[6] L. Torpo, S. Poykko, and R. M. Nieminen, Phys. Rev. B **57**, 6243 (1998).
[7] H. C. Huang, N. M. Ghoniem, J. K. Wong, and M. I. Baskes, Modell. Simul. Mater. Sci. Eng. **3**, 615 (1995).
[8] T. Diaz de la Rubia, J. M. Perlado, and M. Tobin, J. Nucl. Mater. **233–237**, 1096 (1996).
[9] R. Devanathan, W. J. Weber, and T. Diaz de la Rubia, Nucl. Instrum. Methods Phys. Res. B **141**, 118 (1998).
[10] F. Gao and W. J. Weber, Phys. Rev. B **63**, 054101 (2000).
[11] F. Gao and W. J. Weber, J. Appl. Phys. **89**, 4275 (2001).
[12] D. J. Bacon and T. Diaz de la Rubia, J. Nucl. Mater. **216**, 275 (1994).
[13] D. J. Bacon, F. Gao, and Yu. N. Osetsky, J. Nucl. Mater. **276**, 1 (2000).
[14] K. O. Trachenko, M. T. Dove, and E. K. H. Salje, J. Phys.: Con-

dens. Matter **13**, 1947 (2001).
[15] S. H. Vosko, L. Wilk, and M. Nusair, Can. J. Phys. **58**, 1200 (1980).
[16] D. M. Ceperley and B. J. Alder, Phys. Rev. Lett. **45**, 566 (1980).
[17] M. Gell-Mann and K. A. Bruecker, Phys. Rev. **106**, 364 (1957).
[18] E. P. Wigner, Trans. Faraday Soc. **34**, 678 (1938).
[19] R. O. Jons and O. Gunnarsson, Rev. Mod. Phys. **61**, 689 (1989).
[20] E. J. Bylaska, D. A. Dixon, and A. R. Felmy, J. Phys. Chem. **104**, 610 (2000).
[21] D. R. Hamann, Phys. Rev. B **40**, 2980 (1989).
[22] K. Kleinman and D. M. Bylander, Phys. Rev. Lett. **48**, 1425 (1982).
[23] C. J. Brabec, E. B. Andson, B. N. Davidson, S. A. Kajihara, Q. M. Zhang, J. Bernhole, and D. Tomanek, Phys. Rev. B **46**, 7326 (1992).
[24] E. J. Bylaska, P. R. Taylor, R. Kawai, and J. H. Weare, J. Phys. Chem. **100**, 6966 (1996).
[25] E. J. Bylaska and J. H. Weare, Phys. Rev. B **58**, R7488 (1998).
[26] E. J. Bylaska, R. Kawai, and T. H. Weare, J. Chem. Phys. **113**, 6096 (2000).
[27] D. H. Yean and J. R. Riter, Jr., J. Phys. Chem. Solids **32**, 653 (1971).
[28] K. J. Chang and M. L. Cohen, Phys. Rev. B **35**, 8196 (1987).
[29] A. Edelman, T. Arias, and S. T. Smith, SIAM J. Matrix Anal. Appl. **20**, 303 (1998).
[30] F. Gao and D. J. Bacon, Philos. Mag. A **67**, 275 (1993).
[31] J. Tersoff, Phys. Rev. Lett. **64**, 1757 (1990).
[32] J. Tersoff, Phys. Rev. B **49**, 16 349 (1994).
[33] R. Devanathan, T. Diaz de la Rubia, and W. J. Weber, J. Nucl. Mater. **253**, 47 (1998).
[34] J. M. Perlado, L. Malerba, A. Sanchez-Rubio, and T. Diaz de la Rubia, J. Nucl. Mater. **276**, 235 (2000).
[35] R. Devanathan, W. J. Weber, and F. Gao, J. Appl. Phys. **90**, 2303 (2001).